Effect of BBT-877, a novel inhibitor of ATX, on a mouse model of type 1 diabetic nephropathy

Jong Han Lee[1], Phyu Phyu Khin[2,6], GwangHee Lee[3,4], Oh Kyung Lim[5], Hee-Sook Jun[2,6]

[1]Department of Marine Bio and Medical Science, Hanseo University, Seosan, Korea
[2]College of Pharmacy and Gachon Institute of Pharmaceutical Science, Gachon University, Incheon, Korea
[3]Bridge Biotherapeutics Incorporation, Seongnam, Korea
[4]Boostimmune Therapeutics Incorporation, Seongnam, Korea
[5]Department of Rehabilitation Medicine, Gachon University, Incheon, Korea
[6]Lee Gil Ya Cancer and Diabetes Institute, Gachon University, Incheon, Korea

Correspondence to: Jong Han Lee, Hee-Sook Jun; **email:** jhleecw3@hanseo.ac.kr, hsjun@gachon.ac.kr

ABSTRACT

Diabetic nephropathy (DN) is one of the common microvascular complications of diabetes. Autotaxin (ATX) is an enzyme with lysophospholipase D activity, producing lysophosphatidic acid (LPA). LPA signaling has been implicated in renal fibrosis, thereby inducing renal dysfunction. BBT-877 is an orally administered small molecule inhibitor of ATX. However, its effect on DN has not been studied so far. In this study, we investigated the effect of BBT-877, a novel inhibitor of ATX, on the pathogenesis of DN in a mouse model of streptozotocin (STZ)-induced diabetes.

BBT-877 treatment significantly reduced albuminuria, albumin-to-creatinine ratio (ACR), neutrophil gelatinase-associated lipocalin (NGAL), and glomerular volume compared to the STZ-vehicle group. Interestingly, BBT-877 treatment attenuated hyperglycemia and dyslipidemia in STZ-induced diabetes mice. In the liver, the expression levels of β-oxidation-related genes such as PPAR α and CPT1 were significantly decreased in STZ-induced diabetic mice. However, this effect was reversed by BBT-877 treatment. BBT-877 treatment also suppressed mRNA levels of pro-inflammatory cytokines IL-6, MCP-1, and TNF-α and protein levels of fibrotic factors (TGF-β, fibronectin, CTGF, and collagen type I alpha I (COL1A1)) in the kidneys of STZ-induced diabetic mice.

In conclusion, our results indicate that BBT-877 is effective in preventing the pathogenesis of DN by reducing systemic blood glucose levels and inhibiting inflammation and fibrosis in the renal tissue of diabetes mice. These novel findings suggest that inhibition of ATX may be a potential therapeutic target for DN.

INTRODUCTION

A progressive kidney condition called diabetic nephropathy (DN) is one of the common microvascular complications of diabetes and frequently leads to end-stage renal disease (ESRD) in individuals with diabetes. Proteinuria, diabetic glomerular lesions, and a reduction in glomerular filtration rate are well-known pathological features of DN [1, 2]. Hyperglycemia, hypertension, dyslipidemia, and genetic predisposition are major contributors to the development of DN [3, 4]. Hyperglycemia causes renal damage through a variety of mechanisms, including the production of advanced glycation end products and the activation of their receptors, reactive oxygen species generation, and inflammation [5, 6]. In particular, renal inflammation

Table 1. Effect of BBT-877 treatment on physiological parameters of STZ-induced diabetic mice.

Characteristic	CV	SV	S108	S308	S908	S10L
Body weight (g)	26.9 ± 0.7	23.5 ± 0.4[†]	25.0 ± 0.4	24.4 ± 0.4	24.5± 0.4	25.0 ± 0.3
Kidney weight (mg)	297.3 ± 8.5	287.7 ± 5.8	272.8 ± 10.3	286.0 ± 11.1	283.4 ± 6.3	292.8 ±8.7
Liver weight (mg)	1105± 40	1385 ± 59[†]	1255 ± 48	1157 ± 57[‡]	1219 ± 46[‡]	1227 ± 48[‡]
Spleen weight (mg)	54.2 ± 3.16	55.4 ± 3.8	49.3 ± 1.9	47.4 ± 2.1	54.3 ± 2.4	48.4 ± 1.0
Food intake (gig per day)	0.19 ± 0.02	0.30 ± 0.03[†]	0.29 ± 0 .03	0.28 ± 0.03	0.26 ± 0.03	0.31 ± 0.03
Water intake (m/lg per day)	0.014 ± 0.0	0.064 ± 0.0[†]	0.045 ± 0.1$^{p = 0.08}$	0.044 ± 0.0	0.039 ± 0.0[‡]	0.044 ± 0.0[‡]
Urine volume (ml/g per day)	0.046 ± 0.0	0.501 ± 0.1[†]	0.282 ± 0.1$^{p = 0.08}$	0.270 ± 0.1$^{p = 0.07}$	0.252 ± 0.1[‡]	0.329 ± 0.1
Albumin/creatinine ratio (µg/mg)	6.87 ± 0.5	31,94 ± 2.9[†]	21.27 ± 3.4[‡]	21.19 ± 4.3$^{p = 0.06}$	19.36± 3.5[‡]	25.66 ± 3.6

Albumin/creatinine ratio was measured at 4 weeks; other parameters were measured at 8 weeks. Data are displayed as mean ± SEM. Abbreviations: STZ: streptozotocin; HbA1c: glycosylated hemoglobin; CV: control-vehicle; SV: STZ-vehicle; S10B: STZ-10 mg BBT-877; S30B: STZ-30 mg BBT-877; S90B: STZ-90 mg BBT-877; S10L: STZ-10 mg Losartan. [†]$p < 0.01$ vs. CV; [‡]$p < 0.05$ vs. SV, noted p values are vs. SV (n = 8–10).

and fibrosis are important cellular and molecular mechanisms in the pathogenesis of DN [7–9]. Therefore, glycemic control is a well-known treatment for DN [1, 10].

Autotaxin (ATX) is an enzyme with lysophospholipase D activity, producing lysophosphatidic acid (LPA) from lysophospholipids. ATX was originally isolated from a conditioned medium of A2058 human melanoma cells [11] and was later identified as the sole source of extracellular LPA [12]. LPA is a small phospholipid derivative that mediates various cellular processes, such as proliferation, survival, and migration, via its G protein-coupled receptors, LPAR1-6s [13]. In addition, LPA induces cell damage through complex overlapping pathways mediated by the generation of reactive oxygen species, inflammatory cytokines, and fibrosis [14, 15]. In particular, the LPA-LPAR axis plays an important role in the pathogenesis of kidney disease, lung fibrosis, and cancer [16]. Indeed, LPA is increased in the serum and kidney cortex of db/db mice, which are used to model type 2 diabetes and obesity [17, 18]. Similarly, ATX is increased in the fat and kidney tissues of db/db mice [19, 20]. A recent study showed that LPA is significantly increased in the urine of patients with type 2 diabetes exclusively associated with albuminuria [21]. We have also reported that the LPA-LPAR axis can induce pathological alterations in the structure and function of kidney cells by upregulation of renal inflammation and fibrosis [15]. In contrast, LPAR antagonism improved renal function in DN through various mechanisms, such as suppression of oxidative stress and inflammation [15, 22, 23]. ATX inhibition is another potential approach to suppress the LPA-LPAR signaling cascade that may have a beneficial effect on the pathogenesis of DN, similar to the effect of LPAR antagonism.

BBT-877 and PF-8380 are orally available small molecule inhibitors of ATX. Recently, Lee et al. showed that BBT-877 treatment effectively decreased LPA production in *in vitro* and *ex vivo* systems [24]. In addition, several ATX inhibitors, including BBT-877, suppressed fibrosis in bleomycin-induced pulmonary fibrotic mice [25] and in liver fibrotic mice [26]. In particular, BBT-877 was less cytotoxic to various cell types, such as hepatocellular carcinoma cells and normal lung fibroblasts [24]. These exciting observations indicate that BBT-877 may have a potential therapeutic effect on DN by suppressing the ATX-LPA-LPAR signaling-mediated renal inflammation and fibrosis. However, the effect of BBT-877 on DN has not been investigated so far.

In this study, we investigated the effect of BBT-877, a novel inhibitor of ATX, on the pathogenesis of DN in a mouse model of streptozotocin (STZ)-induced diabetes. Our results demonstrated that BBT-877 administration restored kidney dysfunction in diabetic mice by lowering systemic blood glucose and lipid levels as well as reducing inflammation and fibrosis in the kidney.

RESULTS

BBT-877 treatment attenuates hyperglycemia and dyslipidemia in STZ-induced diabetic mice

Body weight significantly decreased in the STZ-vehicle group compared to the control-vehicle group, but this effect was ameliorated by BBT-877 and losartan administration (Table 1). Blood glucose was also remarkably increased in the STZ-vehicle group compared to the control-vehicle group, but this effect was significantly decreased by BBT-877 treatment in a dose-dependent manner (Figure 1A). Although the

losartan group had slightly lower blood glucose levels than the STZ-vehicle mice, the effect was not significant (Figure 1A). The levels of HbA1c displayed a similar trend to that of blood glucose levels, with a dose-dependent response in the BBT-877-treated groups (Figure 1B). In addition, the losartan group had slightly lower HbA1c levels than the STZ-vehicle mice, but the effect was not significant (Figure 1B). Triglyceride and cholesterol levels were significantly increased in the STZ-treated mice (Figure 1C, 1D), and this effect was ameliorated in a dose-dependent manner by BBT-877 administration, and similarly by losartan treatment (Figure 1C, 1D). Furthermore, the weights of tissues, such as the kidney and spleen, which were measured at the end of the experiment, were comparable among the treatment groups (control, STZ-vehicle, and STZ-BBT-

877), except for the liver (Table 1). Although the weight of the liver was increased in the STZ-vehicle group, it decreased in a dose-dependent manner following treatment with BBT-877 (Table 1). In STZ-induced diabetic mice, β-oxidation-related genes of peroxisome proliferator-activated receptor α (*PPAR* α) and carnitine palmitoyltransferase-1 (*CPT1*) were significantly reduced in the liver. However, this effect was reversed by BBT-877 treatment (Supplementary Figure 1). In contrast, the expression levels of the lipogenesis-related genes—fatty acid synthase (FAS) and stearoyl-CoA desaturase-1 (SCD-1)—did not show any statistically significant differences across all groups. Interestingly, the expression of the fatty acid binding protein 4 (FABP4)—a potential biomarker for fat accumulation—significantly increased and reduced
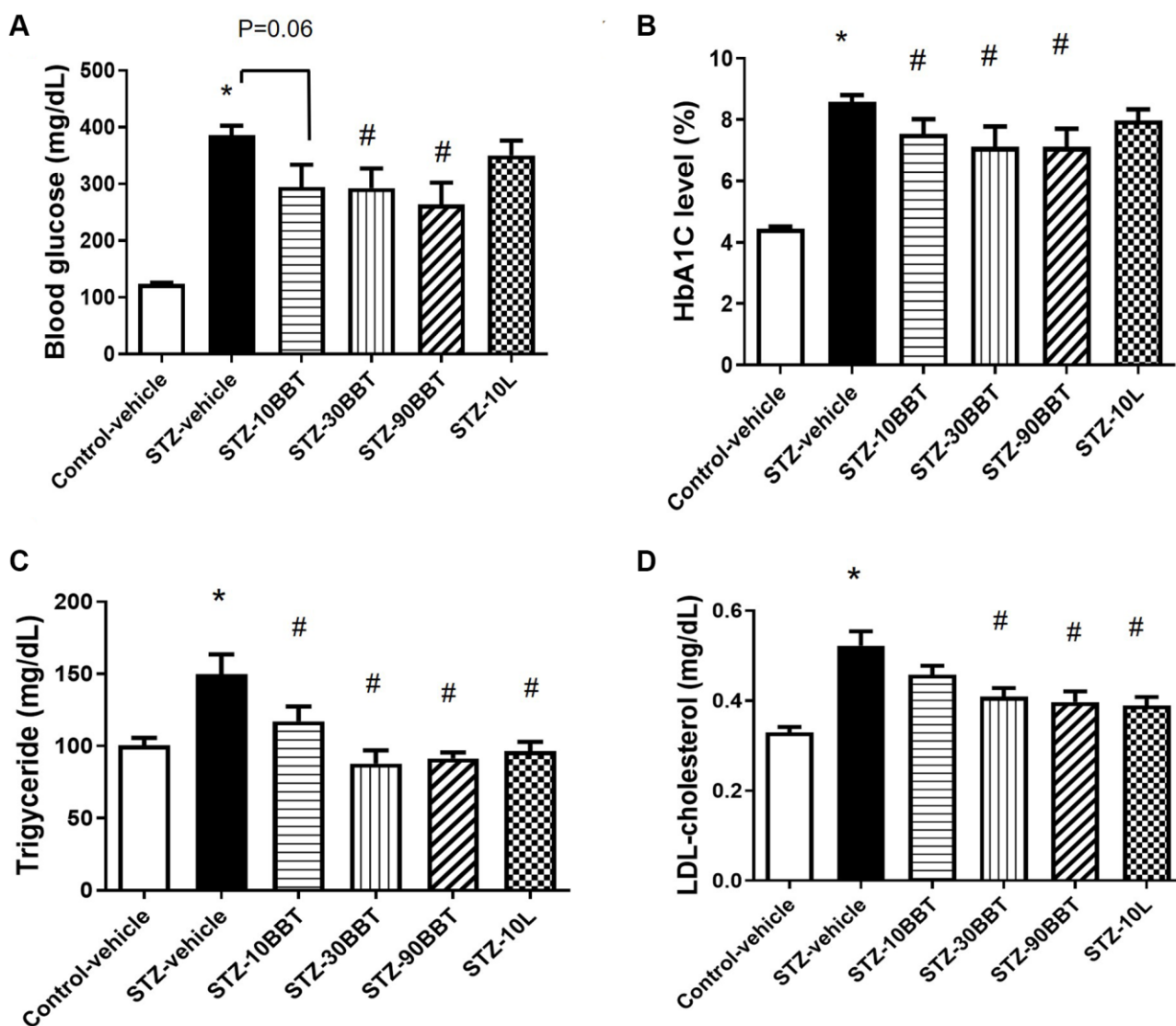

Figure 1. BBT-877 attenuates hyperglycemia and dyslipidemia in STZ-induced diabetic mice. After mice were administered BBT-877 for 8 weeks, measurements were taken for (**A**) blood glucose, (**B**) HbA1c, (**C**) Triglyceride, and (**D**) LDL-cholesterol. Abbreviations: STZ: streptozotocin; HbA1c: glycosylated hemoglobin. STZ-10BBT: BBT-877 10 mg/kg, STZ-30BBT: BBT-877 30 mg/kg, STZ-90BBT: BBT-877 90 mg/kg, STZ-10L: losartan 10 mg/kg. $^*p < 0.05$, control-vehicle vs. STZ-vehicle, $^#p < 0.05$, STZ-vehicle vs. STZ-10, 30, 90BBT or STZ-10L, $n = 8–10$.

by BBT-877 in a dose-dependent manner (Supplementary Figure 1).

BBT-877 treatment improves kidney function in STZ-induced diabetic mice

Food intake was comparable among STZ groups but showed a tendency to decrease in a dose-dependent manner in the STZ-BBT-877 groups, although the difference was not statistically significant (Table 1). Urination and increased water intake were reduced by BBT-877 in a dose-dependent manner in diabetic mice at 4 weeks, compared to the STZ-vehicle group (Table 1). In particular, the reduction in water intake and urination was significant in mice administered with 90 mg/kg BBT-877 (Table 1). Consistently, losartan exerted a similar effect on both parameters, as shown in Table 1. compared to the control-vehicle group, the microalbumin and creatinine ratio (ACR) increased in the diabetic mice at 4 weeks. In contrast, treatment with BBT-877 decreased the ACR ratio in all diabetic groups. The reduction levels were similar and reached statistical significance at both 10 and 90 mg/kg BBT-877 (Table 1). Losartan administration lowered the ACR compared to the STZ-vehicle group but the change was not significantly different (Table 1). Consistently, the concentration of urinary neutrophil gelatinase-associated lipocalin (NGAL) was highly increased in diabetic mice. However, treatment with BBT-877 significantly suppressed the release of NGAL in a dose-dependent manner, indicating that BBT-887 can reverse the diabetes-induced tubular damage of the kidney. In addition, the protein and mRNA expression levels of NGAL were increased in the STZ-vehicle group but suppressed by BBT-877 and losartan, as positive control treatment (Supplementary Figure 2).

BBT-877 treatment reduces glomerular injury in the kidneys of STZ-induced diabetic mice

The glomerular surface area significantly increased in diabetic mice. However, this increase was remarkably decreased by treatment with BBT-877 in a dose-dependent manner (Figure 2A, 2B). Furthermore,
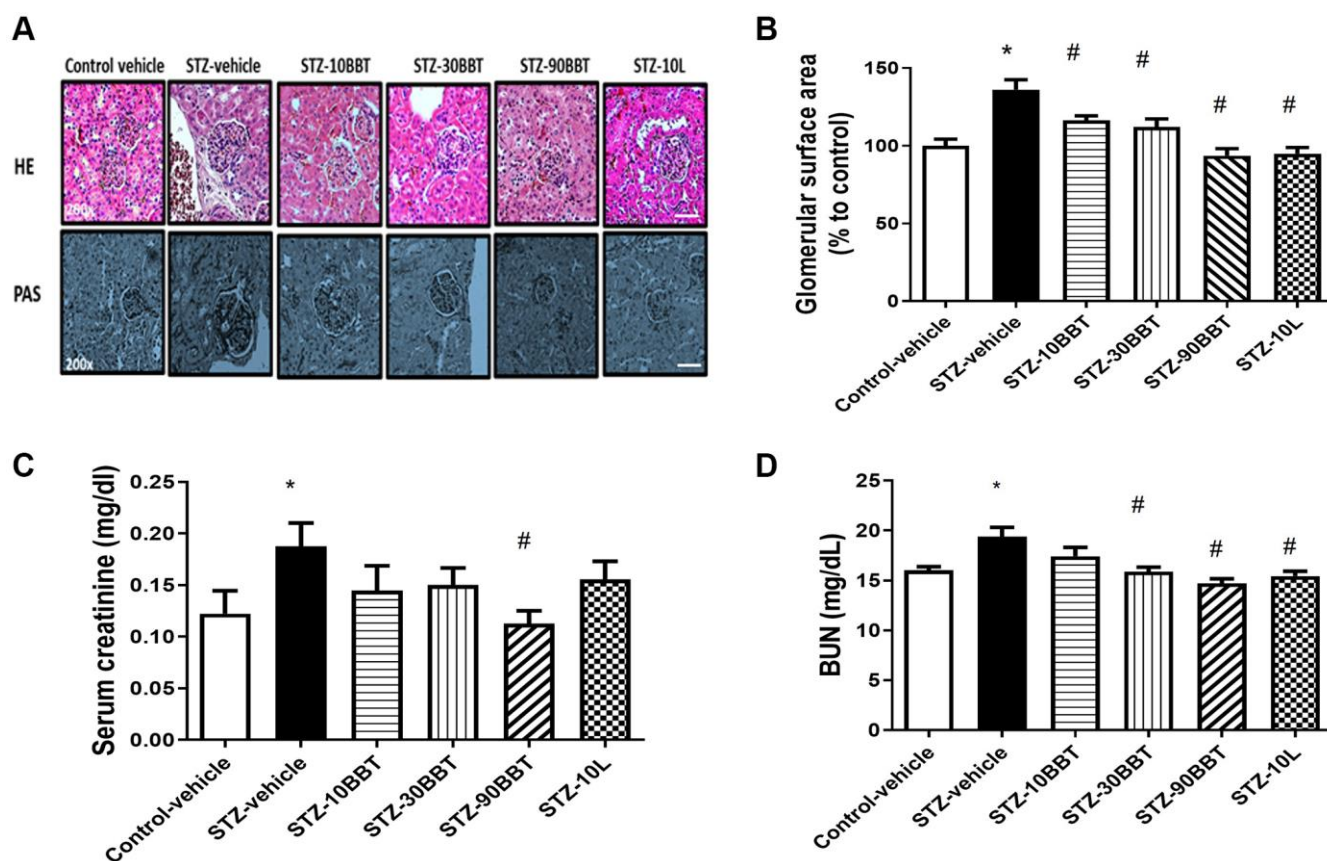
Figure 2. BBT-877 reduces glomerular injury in the kidneys of STZ induced diabetic mice. After treatment with BBT-877 for 8 weeks, mice were sacrificed and their kidneys were collected, fixed in 10% formalin buffer, and embedded in paraffin. The kidney sections were stained with hematoxylin and eosin (HE) and Periodic acid-Schiff (PAS). Glomerular surface area was quantified using 30 glomeruli per mouse by ImageJ Software. (**A**) Representative image of HE and PAS staining, scale bars = 20 μm (**B**) Glomerular surface area, (**C**) Serum creatinine, (**D**) Blood urea nitrogen. Abbreviation: STZ: streptozotocin. STZ-10BBT: BBT-877 10 mg/kg, STZ-30BBT: BBT-877 30 mg/kg, STZ-90BBT: BBT-877 90 mg/kg, STZ-10L: losartan 10 mg/kg. $^*p < 0.05$, control-vehicle vs. STZ-vehicle, $^#p < 0.05$, STZ-vehicle vs. STZ-10, 30, 90BBT or STZ-10L, $n = 8–10$.

the glomerular surface area was comparable between the high-BBT-877 and losartan treatment groups (Figure 2A, 2B). Since creatinine and BUN are known biomarkers of renal function, we measured their serum levels after 8 weeks of BBT-877 administration. Serum creatinine levels were increased in STZ-vehicle mice but decreased by BBT-877. Furthermore, a statistically significant difference was observed following the administration of 90 mg/kg BBT-877 (Figure 2C). Similarly, 10 mg/kg losartan attenuated this increase, but did not differ significantly from the STZ-vehicle group (Figure 2C). BUN levels were also increased in the STZ-vehicle group compared to the control-vehicle mice, and this was also significantly decreased by BBT-877 and losartan (Figure 2D).

BBT-877 treatment inhibits the expression of pro-inflammatory cytokines and fibrotic factors in the kidneys of STZ-induced diabetic mice

To determine whether BBT-877 treatment modulates the expression of pro-inflammatory cytokines and fibrotic factors in the kidneys of STZ-induced diabetic mice, we measured the mRNA expression of inflammatory cytokines and the protein expression of fibrotic factors. The expression levels of interleukin 6 (IL-6), tumor necrosis factor-α (TNF-α), and monocyte chemoattractant protein-1 (MCP-1) were significantly increased in STZ-induced diabetic mice; however, this increase was suppressed in a dose-dependent manner by BBT-877 administration (Figure 3). Losartan treatment also suppressed inflammatory cytokine expression to a level similar to the highest dose of BBT-877 (Figure 3). Consistent with these findings, TGF-β expression level was increased in STZ-induced diabetic mice; however, this increase was reduced by BBT-877, again in a dose-dependent manner, with a statistically significant difference observed with 90 mg/kg BBT-877 (Figure 4A). Similarly, the expression level of fibronectin was upregulated in the STZ-vehicle group compared to the control-vehicle group. However, both BBT-877 (90 mg/kg) and losartan (10 mg/kg) remarkably suppressed its expression (Figure 4B). The expression level of CTGF was significantly reduced in all treatment groups, including the losartan group, compared to the STZ-vehicle group (Figure 4C). Moreover, COL1A1 protein
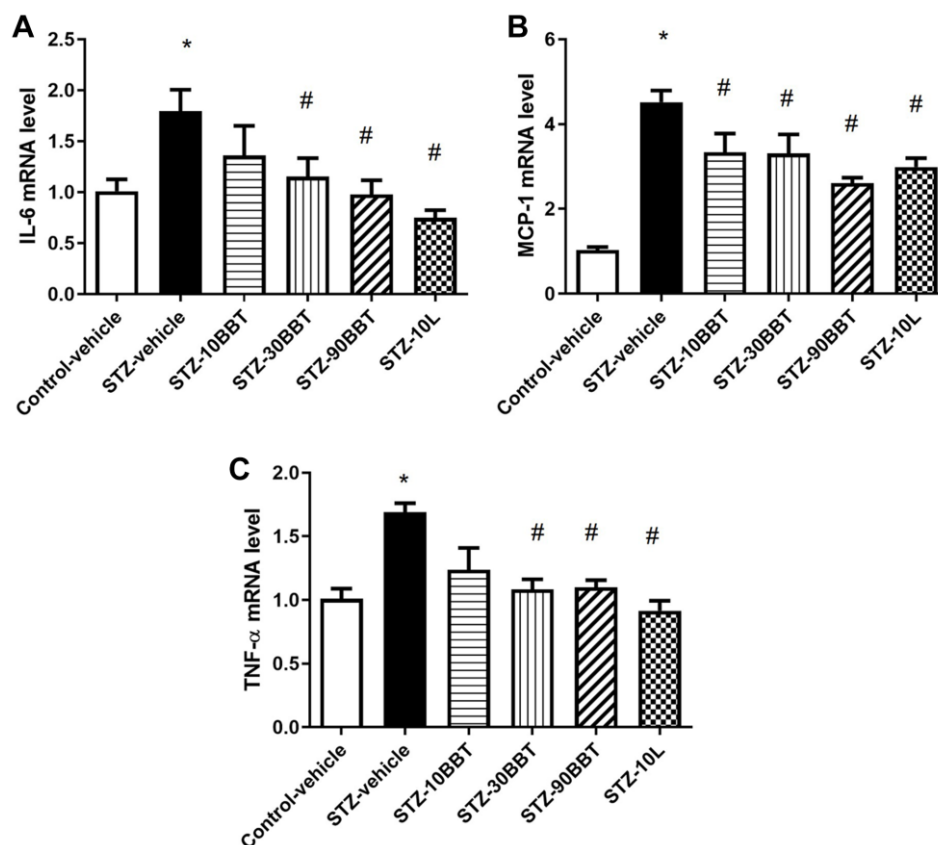

Figure 3. BBT-877 reduces the mRNA levels of inflammatory cytokines in STZ-induced diabetic mice. After treatment with BBT-877 for 8 weeks, mice were sacrificed and their kidneys were collected. RNA was extracted and subjected to qRT-PCR for (**A**) IL-6, (**B**) MCP-1, and (**C**) TNF-α. Abbreviations: STZ: streptozotocin; qRT-PCR: quantitative reverse transcriptase-polymerase chain reaction. STZ-10BBT: BBT-877 10 mg/kg, STZ-30BBT: BBT-877 30 mg/kg, STZ-90BBT: BBT-877 90 mg/kg, STZ-10L: losartan 10 mg/kg. $^*p < 0.05$, control-vehicle vs. STZ-vehicle, $^\#p < 0.05$, STZ-vehicle vs. STZ-10, 30, 90BBT or STZ-10L, $n = 8–10$.

expression levels were significantly decreased by treatment with 90 mg BBT-877 (Figure 4D).

DISCUSSION

We and others have shown that LPAR antagonism improves renal dysfunction in both type 1 and type 2 diabetic rodent models [15, 22, 23]. Here, we demonstrated that BBT-877, a novel inhibitor of ATX, attenuates DN in type 1 diabetic mice by lowering systemic blood glucose levels as well as suppressing the expression of pro-inflammatory cytokines and fibrotic factors in the kidney.

ATX is an enzyme responsible for LPA production. The ATX-LPA-LPAR axis is involved in the pathogenesis and progression of DN, including glomerulosclerosis, tubulointerstitial fibrosis (TIF), and changes in renal vasculature [27]. Serum ATX and LPA levels are associated with increased proteinuria and kidney failure in type 2 diabetes patients [28]. In addition, LPAR1-4 are expressed in kidney tissue under normal conditions, and LPAR 1 and 3 are further elevated in diabetic conditions [22]. Our previous studies and those of others demonstrated that inhibition of the LPA-LPAR axis by LPA receptor antagonists (such as ki16425, AM095, and BMS002) attenuates kidney dysfunction
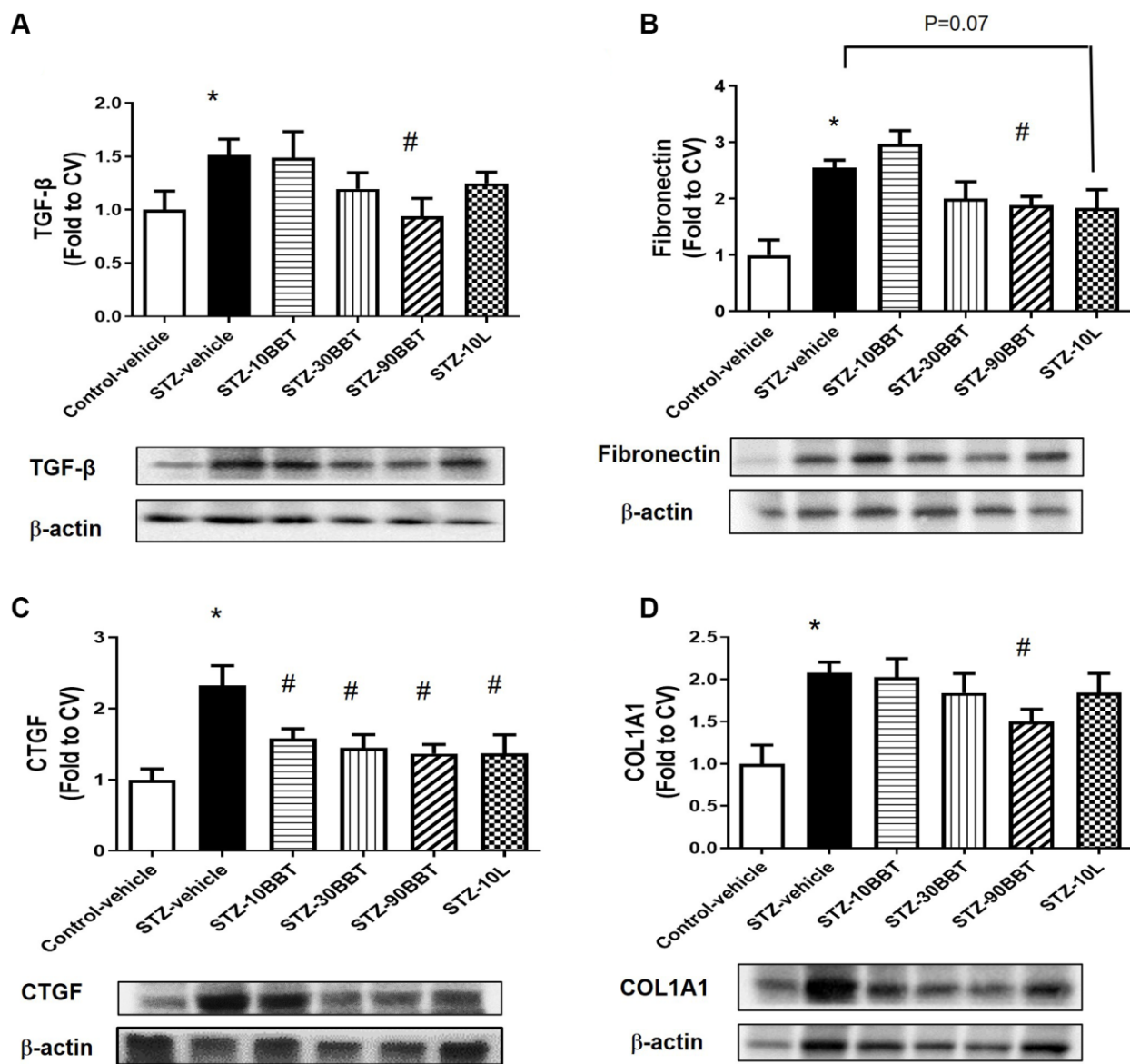

Figure 4. BBT-877 reduces the protein levels of fibrotic factors in STZ-induced diabetic mice. After treatment with BBT-877 for 8 weeks, mice were sacrificed and their kidneys were collected. Protein was extracted and subjected to western blotting for (**A**) TGF-β, (**B**) Fibronectin, (**C**) CTGF, and (**D**) COL1A1. Abbreviations: STZ: streptozotocin; qRT-PCR: quantitative reverse transcriptase-polymerase chain reaction. STZ-10BBT: BBT-877 10 mg/kg, STZ-30BBT: BBT-877 30 mg/kg, STZ-90BBT: BBT-877 90 mg/kg, STZ-10L: losartan 10 mg/kg. $^*p < 0.05$, control-vehicle vs. STZ-vehicle, $^\#p < 0.05$, STZ-vehicle vs. STZ-10, 30, 90BBT or STZ-10L, $n = 8–10$.

through various cellular and molecular mechanisms, including anti-oxidant, anti-inflammatory, and anti-fibrotic effects [15, 22, 23].

BBT-877 is an orally available small molecule inhibitor of ATX that mimics LPA receptor antagonism, leading to the suppression of fibrosis in lung tissue [24, 29]. Our current data reveal that BBT-877 administration similarly attenuates kidney hyperfiltration and kidney dysfunction in diabetic states, as revealed by the reduced water intake, urination, and ACR compared to the STZ-vehicle group, respectively. These data are consistent with a study showing that another ATX inhibitor, PF-8380, ameliorated progressive proteinuria and TIF in chronic allograft injury in rats [30].

Consistently, the biomarkers of kidney dysfunction, including serum creatinine, BUN, and urinary NGAL, improved in a dose-dependent manner, while glomerular volume reduced in the BBT-877-treated STZ-induced diabetic mice. Additionally, BBT-877 reduced blood glucose and HbA1c levels without changing the body weight of mice. These findings could explain how the administration of BBT-877 recovers kidney dysfunction. Similarly, several studies have shown that glycemic control significantly attenuates microalbuminuria and proteinuria, as well as reduces kidney dysfunction in diabetes patients [31–33]. In alignment with the previous results from our group and others, losartan did not attenuate the blood glucose and HbA1c levels, despite the reduction trend identified following its administration [15, 22, 34].

In ATX null and adipocyte-specific ATX knockout mice, they showed smaller body weight gains and less insulin resistance under high fat diet feeding by suppressing adipose tissue expansion [35]. Similarly, lowering LPA level by BBT-877 administration may indirectly affect to key peripheral tissues associated with systemic insulin sensitivity, including the liver, fat tissue, and pancreas. Indeed, BBT-877 treatment group mice had significantly lighter liver than SV group mice. The expression levels of several genes in the liver (such as *PPAR α, CPT1* involved in β-oxidation, and *FABP4* involved in triglyceride synthesis and its accumulation) in the SV group indicated fat accumulation. This possibly impairs liver function associated with glycemic control.

In contrast, the levels of triglyceride and LDL-cholesterol were significantly reduced in the BBT-877 treatment groups compared to that in the SV group. Reduced TG and LDL-cholesterol in serum by BBT-877 treatment may also enhance systemic insulin sensitivity by attenuating lipotoxicity in peripheral tissues and/or by suppressing systemic and local inflammation levels. Collectively, these beneficial effects of BBT-877 on insulin sensitivity may attenuate DN. However, the current study does not cover the detailed molecular mechanism by which BBT-877 regulates blood glucose and lipid levels. Therefore, further studies are needed to elucidate the precise molecular mechanisms involved in key peripheral tissues.

Inflammatory cytokines and fibrotic factors play important roles in the progression of DN [22, 36, 37]. Although fibrosis allows normal wound healing and injury repair in the maintenance of various normal tissues [38], acute or chronic injurious stimuli can cause a dysregulation of normal healing processes. This can lead to excess deposition of the extracellular matrix and fibrosis, and a complex multistage inflammatory process, which ultimately results in cell death and tissue injury [39, 40]. Several studies have shown that activation of the LPA-LPAR axis increases the expression of renal inflammatory cytokines [16, 22, 41]. Similarly, diabetic mice had significantly higher mRNA expression levels of IL-6, TNF-α, and MCP-1 than control mice. However, these levels were significantly suppressed by BBT-877 treatment.

TGF-β is the central cellular effector of fibrotic responses and may also promote a fibrogenic phenotype in various cells, such as immune and vascular cells [42]. Toll-like receptor signaling, oxidative stress, and proinflammatory cytokines (such as IL-1β, TNF-α, and IL-6) can stimulate the transcription of TGF-β isoforms in fibrotic tissues [15, 43, 44]. Recently, Lee et al. showed that BBT-877 attenuated fibrosis in a mouse model of bleomycin-induced pulmonary fibrosis [24]. Consistently, our data also showed that TGF-β expression was significantly increased with the expression levels of fibrotic factors, including fibronectin, CTGF, and COL1A1 in diabetic mice. However, these increases in expression were significantly inhibited by BBT-877 treatment.

In conclusion, our study demonstrates that BBT-877 may reduce blood glucose levels and suppress the expression of inflammatory cytokines and fibrotic factors in the kidney, thereby improving kidney dysfunction in type 1 diabetic mice. Based on our findings, we conclude that there are two different mechanisms by which BBT-877 indirectly enhances insulin sensitivity and attenuates lipotoxicity in peripheral tissues, as well as directly suppresses inflammation and fibrosis in the kidney. Therefore, ATX inhibition could be another potential approach for LPA-LPAR antagonism and could be a potential target for therapeutic strategies to slow the progression of DN.

MATERIALS AND METHODS

Animals

Eight-week-old male C57BL/6N mice ($n = 50$) with similar body weights were used to establish an STZ-induced diabetic mouse model. Briefly, the mice were randomly divided into control and STZ groups, and mice in the latter group were intraperitoneally administered 50 mg/kg STZ after fasting for 4 h in the morning, once daily for 5 days. Citrate buffer (pH 4.5) was injected according to the body weight of each mouse to serve as a control. Blood glucose levels were monitored every 3 days for 2 weeks following STZ injection. Diabetes was confirmed by a blood glucose level of > 320 mg/dl. After the establishment of the STZ-induced diabetic mouse model, animals with similar body weights were randomly divided into the following groups ($n = 8$−10 mice per group): STZ-vehicle, STZ-BBT-877, and STZ-losartan. Age-matched non-diabetic mice were used as controls. BBT-877 was freshly prepared immediately before administration, according to the instructions provided by Bridge Biotherapeutics, Inc. BBT-877 was orally administered every day in the morning (09:00) and in the evening (19:00) at doses of 10 mg/kg, 30 mg/kg, and 90 mg/kg for 8 weeks. Mice in the losartan group were orally administered a dose of 10 mg/kg every day in the morning (09:00) and vehicle solution (PEG200 + 0.5% methylcellulose (400 cp) at a 1:3 volume ratio) in the evening (19:00) for 8 weeks. All procedures were approved by the Institutional Animal Care and Use Committee of the Gachon University.

Biochemical parameters in blood and urine

Four weeks after the administration of BBT-877, losartan, or vehicle control, mice were housed in individual metabolic cages for 24 h allowing measurement of food intake, water intake, and urine volume. Urine was collected and, after debris removal via gentle centrifugation at 2,000 rpm for 5 min, stored at −80°C until analysis. All parameters, such as creatinine and microalbumin, were measured by Knotus Co., Ltd. (Incheon, Korea). Urinary neutrophil gelatinase-associated lipocalin (NGAL) was measured using a commercially available mouse ELISA kit (Abcam, ab119601) according to the manufacturer instructions. NGAL concentrations were normalized to urinary creatinine concentrations. Blood was collected via the tail vein and non-fasting glucose levels were measured using a glucose analyzer (One Touch®Ultra, LifeScan Johnson&Johnson, Milpitas, CA, USA) every week for 8 weeks. Hemoglobin A1c (HbA1c) was detected from blood using a DCA System HbA1c Reagent Kit (Siemens, New York, NY, USA) 8 weeks after drug treatment. Blood was also collected at the end of the experiment, immediately after sacrificing, and centrifuged at 10,000 rpm and then 5,000 rpm, each for 10 min. Finally, the supernatants were collected and stored at −80°C until analysis. The serum levels of blood urea nitrogen (BUN), creatinine, cholesterol, and triglycerides were assessed by the Southeast Medi-Chem Institute.

Renal histological assessment

After 8 weeks of treatment with BBT-877, the mice were sacrificed and their kidneys were harvested, rapidly collected, and weighted. The left kidney was fixed in 10% formalin buffer and embedded in paraffin. Sections were stained with hematoxylin and eosin, and the glomerular structure was observed under a light microscope. The sections were also stained with the periodic acid-Schiff kit (Sigma-Aldrich, St. Louis, MO, USA), according to the manufacturer's instructions. Images of the glomerulus were acquired under a microscope at 200× magnification. Glomerular volumes were analyzed using the ImageJ program (NIH, Bethesda, MD, USA), with up to 30 glomeruli from each mouse.

Western blotting

Total protein was isolated from tissues using mammalian protein extract buffer (GE Life Science, 28-9712-79) containing a protease inhibitor cocktail (Sigma-Aldrich, P8340). Equal quantities of protein were separated and transferred onto polyvinylidene fluoride membranes. The membranes were then incubated with one of the following antibodies, as appropriate, at a concentration of 1 in 1,000: anti-β-actin (Cell Signaling, #8457), fibronectin (Santa Cruz, sc-8422), COL1A1 (Santa Cruz, sc-293182), CTGF (Santa Cruz, sc-101586), TGF-β (Cell Signaling, #3711), and anti-lipocalin-2/NGAL antibody (Abcam, ab63929). The density of each band was quantified using ImageJ and normalized to β-actin.

Quantitative reverse transcriptase-polymerase chain reaction (qRT-PCR)

Total RNA was extracted from the kidney tissue of the STZ-induced diabetic mouse model using TRIzol reagent (TAKARA). cDNA was synthesized from 2 μg of total RNA using the PrimeScript 1st strand cDNA synthesis kit (TAKARA, 6110A). Real-time qRT-PCR was performed using the Applied Biosystems Prism 7900HT Real-Time PCR system. Relative gene expression levels were normalized to cyclophilin A RNA. The primers used for qRT-PCR were as follows: IL6-forward primer, 5′TCCAGTTGCCTTCTT GGGACTGAT3′, reverse primer, 5′AGCCTCC

GACTTGTCAAGTGGTAT3′, MCP-1-forward primer, 5′GCAGTTAACGCCCCACTCA3′, reverse primer, 5′CCAGCCTACTCATTGGGATCA3′, TNF-α-forward primer, 5′CCAACGGCATGGATCTCAAAGACA3′, reverse primer, 5′AGATAGCAAATCGGCTGACGGTGT3′, PPAR α-forward primer, 5′TATTCGGCTGAAGCTGGTGTAC3′, reverse primer, 5′CTGGCATTTGTTCCGGTTCT3′, CPT-1-forward primer, 5′CAAAGATCAATCGGACCCTAGAC3′, reverse primer, 5′CGCCACTCACGATGTTCTTC3′, FAS-forward primer, 5′CGCCACTCACGATGTTCTTC3′, reverse primer, 5′AGAGACGTGTCACTCCTGGACTT3′, SCD-1-forward primer, 5′CCGGAGACCCTTAGATCGA3′, reverse primer, 5′TAGCCTGTAAAAGATTTCTGCAAACC3′, FABP-4 forward primer, 5′ACACCGAGATTTCCTTCAAACTG3′, reverse primer, 5′CCATCTAGGGTTATGATGCTCTTCA3′, NGAL forward primer, 5′GGCAGCTTTACGATGTACAGCA3′, reverse primer, 5′TCTGATCCAGTAGCGACAGCC3′.

Statistical analysis

All results are expressed as mean ± SEM. Differences between more than two groups were analyzed using one-way ANOVA followed by Scheffe's post-hoc multiple comparison test. Statistical significance was set at $p < 0.05$.

AUTHOR CONTRIBUTIONS

J.H.L designed, conducted experiments, performed data analysis, and wrote the manuscript. P.P.K conducted experiments and performed data analysis. GH. L. and O.K.L. critiqued and edited the paper. H.S.J designed the study, interpreted the data, wrote the manuscript, and approved the final version of the manuscript for publication. All authors read and approved the final manuscript.

CONFLICTS OF INTEREST

The authors declare that they have no conflicts of interest. Bridge Biotherapeutics was the sponsor of the study. GwangHee Lee is employee of Bridge Biotherapeutics.

ETHICAL STATEMENT

All animal experiments were performed under the Institutional Animal Care and Use Committee (IACUC) protocol approved by the Gachon University.

REFERENCES

1. Drummond K, Mauer M, and International Diabetic Nephropathy Study Group. The early natural history of nephropathy in type 1 diabetes: II. Early renal structural changes in type 1 diabetes. Diabetes. 2002; 51:1580–7.
   https://doi.org/10.2337/diabetes.51.5.1580
   PMID:11978659

2. Lim A Kh. Diabetic nephropathy - complications and treatment. Int J Nephrol Renovasc Dis. 2014; 7:361–81.
   https://doi.org/10.2147/IJNRD.S40172
   PMID:25342915

3. Gross JL, de Azevedo MJ, Silveiro SP, Canani LH, Caramori ML, Zelmanovitz T. Diabetic nephropathy: diagnosis, prevention, and treatment. Diabetes Care. 2005; 28:164–76.
   https://doi.org/10.2337/diacare.28.1.164
   PMID:15616252

4. Scott LJ, Warram JH, Hanna LS, Laffel LM, Ryan L, Krolewski AS. A nonlinear effect of hyperglycemia and current cigarette smoking are major determinants of the onset of microalbuminuria in type 1 diabetes. Diabetes. 2001; 50:2842–9.
   https://doi.org/10.2337/diabetes.50.12.2842
   PMID:11723069

5. Schena FP, Gesualdo L. Pathogenetic mechanisms of diabetic nephropathy. J Am Soc Nephrol. 2005 (Suppl 1); 16:S30–3.
   https://doi.org/10.1681/asn.2004110970
   PMID:15938030

6. Wolf G. New insights into the pathophysiology of diabetic nephropathy: from haemodynamics to molecular pathology. Eur J Clin Invest. 2004; 34:785–96.
   https://doi.org/10.1111/j.1365-2362.2004.01429.x
   PMID:15606719

7. Barutta F, Bruno G, Grimaldi S, Gruden G. Inflammation in diabetic nephropathy: moving toward clinical biomarkers and targets for treatment. Endocrine. 2015; 48:730–42.
   https://doi.org/10.1007/s12020-014-0437-1
   PMID:25273317

8. Liu Y. Renal fibrosis: new insights into the pathogenesis and therapeutics. Kidney Int. 2006; 69:213–7.
https://doi.org/10.1038/sj.ki.5000054
PMID:16408108

9. Gagliardini E, Benigni A. Role of anti-TGF-beta antibodies in the treatment of renal injury. Cytokine Growth Factor Rev. 2006; 17:89–96.
https://doi.org/10.1016/j.cytogfr.2005.09.005
PMID:16257566

10. Alicic RZ, Rooney MT, Tuttle KR. Diabetic Kidney Disease: Challenges, Progress, and Possibilities. Clin J Am Soc Nephrol. 2017; 12:2032–45.
https://doi.org/10.2215/CJN.11491116
PMID:28522654

11. Stracke ML, Krutzsch HC, Unsworth EJ, Arestad A, Cioce V, Schiffmann E, Liotta LA. Identification, purification, and partial sequence analysis of autotaxin, a novel motility-stimulating protein. J Biol Chem. 1992; 267:2524–9.
PMID:1733949

12. van Meeteren LA, Ruurs P, Stortelers C, Bouwman P, van Rooijen MA, Pradère JP, Pettit TR, Wakelam MJ, Saulnier-Blache JS, Mummery CL, Moolenaar WH, Jonkers J. Autotaxin, a secreted lysophospholipase D, is essential for blood vessel formation during development. Mol Cell Biol. 2006; 26:5015–22.
https://doi.org/10.1128/MCB.02419-05
PMID:16782887

13. Sheng X, Yung YC, Chen A, Chun J. Lysophosphatidic acid signalling in development. Development. 2015; 142:1390–5.
https://doi.org/10.1242/dev.121723
PMID:25852197

14. Dumas SJ, Meta E, Borri M, Luo Y, Li X, Rabelink TJ, Carmeliet P. Phenotypic diversity and metabolic specialization of renal endothelial cells. Nat Rev Nephrol. 2021; 17:441–64.
https://doi.org/10.1038/s41581-021-00411-9
PMID:33767431

15. Lee JH, Sarker MK, Choi H, Shin D, Kim D, Jun HS. Lysophosphatidic acid receptor 1 inhibitor, AM095, attenuates diabetic nephropathy in mice by downregulation of TLR4/NF-κB signaling and NADPH oxidase. Biochim Biophys Acta Mol Basis Dis. 2019; 1865:1332–40.
https://doi.org/10.1016/j.bbadis.2019.02.001
PMID:30763641

16. Lee JH, Kim D, Oh YS, Jun HS. Lysophosphatidic Acid Signaling in Diabetic Nephropathy. Int J Mol Sci. 2019; 20:2850.
https://doi.org/10.3390/ijms20112850
PMID:31212704

17. Rancoule C, Attané C, Grès S, Fournel A, Dusaulcy R, Bertrand C, Vinel C, Tréguer K, Prentki M, Valet P, Saulnier-Blache JS. Lysophosphatidic acid impairs glucose homeostasis and inhibits insulin secretion in high-fat diet obese mice. Diabetologia. 2013; 56:1394–402.
https://doi.org/10.1007/s00125-013-2891-3
PMID:23508306

18. Hirata T, Smith SV, Takahashi T, Miyata N, Roman RJ. Increased Levels of Renal Lysophosphatidic Acid in Rodent Models with Renal Disease. J Pharmacol Exp Ther. 2021; 376:240–9.
https://doi.org/10.1124/jpet.120.000353
PMID:33277348

19. Grove KJ, Voziyan PA, Spraggins JM, Wang S, Paueksakon P, Harris RC, Hudson BG, Caprioli RM. Diabetic nephropathy induces alterations in the glomerular and tubule lipid profiles. J Lipid Res. 2014; 55:1375–85.
https://doi.org/10.1194/jlr.M049189
PMID:24864273

20. Ferry G, Tellier E, Try A, Grés S, Naime I, Simon MF, Rodriguez M, Boucher J, Tack I, Gesta S, Chomarat P, Dieu M, Raes M, et al. Autotaxin is released from adipocytes, catalyzes lysophosphatidic acid synthesis, and activates preadipocyte proliferation. Up-regulated expression with adipocyte differentiation and obesity. J Biol Chem. 2003; 278:18162–9.
https://doi.org/10.1074/jbc.M301158200
PMID:12642576

21. Saulnier-Blache JS, Feigerlova E, Halimi JM, Gourdy P, Roussel R, Guerci B, Dupuy A, Bertrand-Michel J, Bascands JL, Hadjadj S, Schanstra JP. Urinary lysophopholipids are increased in diabetic patients with nephropathy. J Diabetes Complications. 2017; 31:1103–8.
https://doi.org/10.1016/j.jdiacomp.2017.04.024
PMID:28506691

22. Li HY, Oh YS, Choi JW, Jung JY, Jun HS. Blocking lysophosphatidic acid receptor 1 signaling inhibits diabetic nephropathy in db/db mice. Kidney Int. 2017; 91:1362–73.
https://doi.org/10.1016/j.kint.2016.11.010
PMID:28111010

23. Zhang MZ, Wang X, Yang H, Fogo AB, Murphy BJ, Kaltenbach R, Cheng P, Zinker B, Harris RC. Lysophosphatidic Acid Receptor Antagonism Protects against Diabetic Nephropathy in a Type 2 Diabetic Model. J Am Soc Nephrol. 2017; 28:3300–11.
https://doi.org/10.1681/ASN.2017010107
PMID:28739650

24. Lee G, Kang SU, Ryou JH, Lim JJ, Lee DY, Kwon HJ, Ha GH, Lee YH. BBT-877, a Potent Autotaxin

Inhibitor in Clinical Development to Treat Idiopathic Pulmonary Fibrosis. Am J Respir Crit Care Med. 2019; 199:A2577.
https://doi.org/10.1164/ajrccm-conference.2019.199.1_MeetingAbstracts.A2577

25. Ninou I, Kaffe E, Müller S, Budd DC, Stevenson CS, Ullmer C, Aidinis V. Pharmacologic targeting of the ATX/LPA axis attenuates bleomycin-induced pulmonary fibrosis. Pulm Pharmacol Ther. 2018; 52:32–40.
https://doi.org/10.1016/j.pupt.2018.08.003
PMID:30201409

26. Bain G, Shannon KE, Huang F, Darlington J, Goulet L, Prodanovich P, Ma GL, Santini AM, Stein AJ, Lonergan D, King CD, Calderon I, Lai A, et al. Selective Inhibition of Autotaxin Is Efficacious in Mouse Models of Liver Fibrosis. J Pharmacol Exp Ther. 2017; 360:1–13.
https://doi.org/10.1124/jpet.116.237156
PMID:27754931

27. Pradère JP, Gonzalez J, Klein J, Valet P, Grès S, Salant D, Bascands JL, Saulnier-Blache JS, Schanstra JP. Lysophosphatidic acid and renal fibrosis. Biochim Biophys Acta. 2008; 1781:582–7.
https://doi.org/10.1016/j.bbalip.2008.04.001
PMID:18455518

28. Shimizu M, Furuichi K, Toyama T, Yamahana J, Ohkawa R, Igarashi K, Aoki J, Kaneko S, Yatomi Y, Wada T. Serum Autotaxin Levels Are Associated with Proteinuria and Kidney Lesions in Japanese Type 2 Diabetic Patients with Biopsy-proven Diabetic Nephropathy. Intern Med. 2016; 55:215–21.
https://doi.org/10.2169/internalmedicine.55.5473
PMID:26831013

29. Zulfikar S, Mulholland S, Adamali H, Barratt SL. Inhibitors of the Autotaxin-Lysophosphatidic Acid Axis and Their Potential in the Treatment of Interstitial Lung Disease: Current Perspectives. Clin Pharmacol. 2020; 12:97–108.
https://doi.org/10.2147/CPAA.S228362
PMID:32765123

30. Cortinovis M, Aiello S, Mister M, Conde-Knape K, Noris M, Novelli R, Solini S, Rodriguez Ordonez PY, Benigni A, Remuzzi G. Autotaxin Inhibitor Protects from Chronic Allograft Injury in Rat Kidney Allotransplantation. Nephron. 2020; 144:38–48.
https://doi.org/10.1159/000502908
PMID:31550726

31. Nathan DM, Genuth S, Lachin J, Cleary P, Crofford O, Davis M, Rand L, Siebert C, and Diabetes Control and Complications Trial Research Group. The effect of intensive treatment of diabetes on the development and progression of long-term complications in insulin-dependent diabetes mellitus. N Engl J Med. 1993; 329:977–86.
https://doi.org/10.1056/NEJM199309303291401
PMID:8366922

32. Writing Team for the Diabetes Control and Complications Trial/Epidemiology of Diabetes Interventions and Complications Research Group. Sustained effect of intensive treatment of type 1 diabetes mellitus on development and progression of diabetic nephropathy: the Epidemiology of Diabetes Interventions and Complications (EDIC) study. JAMA. 2003; 290:2159–67.
https://doi.org/10.1001/jama.290.16.2159
PMID:14570951

33. Fioretto P, Bruseghin M, Berto I, Gallina P, Manzato E, Mussap M. Renal protection in diabetes: role of glycemic control. J Am Soc Nephrol. 2006; 17:S86–9.
https://doi.org/10.1681/ASN.2005121343
PMID:16565255

34. Laakso M, Karjalainen L, Lempiäinen-Kuosa P. Effects of losartan on insulin sensitivity in hypertensive subjects. Hypertension. 1996; 28:392–6.
https://doi.org/10.1161/01.hyp.28.3.392
PMID:8794822

35. Nishimura S, Nagasaki M, Okudaira S, Aoki J, Ohmori T, Ohkawa R, Nakamura K, Igarashi K, Yamashita H, Eto K, Uno K, Hayashi N, Kadowaki T, et al. ENPP2 contributes to adipose tissue expansion and insulin resistance in diet-induced obesity. Diabetes. 2014; 63:4154–64.
https://doi.org/10.2337/db13-1694
PMID:24969110

36. Blázquez-Medela AM, López-Novoa JM, Martínez-Salgado C. Mechanisms involved in the genesis of diabetic nephropathy. Curr Diabetes Rev. 2010; 6:68–87.
https://doi.org/10.2174/157339910790909422
PMID:20041836

37. Borthwick LA, Wynn TA, Fisher AJ. Cytokine mediated tissue fibrosis. Biochim Biophys Acta. 2013; 1832:1049–60.
https://doi.org/10.1016/j.bbadis.2012.09.014
PMID:23046809

38. White ES, Mantovani AR. Inflammation, wound repair, and fibrosis: reassessing the spectrum of tissue injury and resolution. J Pathol. 2013; 229:141–4.
https://doi.org/10.1002/path.4126
PMID:23097196

39. Le Saux CJ, Chapman HA. Idiopathic Pulmonary Fibrosis: Cell Death and Inflammation Revisited. Am J Respir Cell Mol Biol. 2018; 59:137–8.
https://doi.org/10.1165/rcmb.2018-0083ED
PMID:29698615

40. Lee SB, Kalluri R. Mechanistic connection between inflammation and fibrosis. Kidney Int Suppl. 2010; S22–6.
https://doi.org/10.1038/ki.2010.418
PMID:21116313

41. Park F, Miller DD. Role of lysophosphatidic acid and its receptors in the kidney. Physiol Genomics. 2017; 49:659–66.
https://doi.org/10.1152/physiolgenomics.00070.2017
PMID:28939644

42. Frangogiannis N. Transforming growth factor-β in tissue fibrosis. J Exp Med. 2020; 217:e20190103.
https://doi.org/10.1084/jem.20190103
PMID:32997468

43. Leemans JC, Butter LM, Pulskens WP, Teske GJ, Claessen N, van der Poll T, Florquin S. The role of Toll-like receptor 2 in inflammation and fibrosis during progressive renal injury. PLoS One. 2009; 4:e5704.
https://doi.org/10.1371/journal.pone.0005704
PMID:19479087

44. Vivekananda J, Lin A, Coalson JJ, King RJ. Acute inflammatory injury in the lung precipitated by oxidant stress induces fibroblasts to synthesize and release transforming growth factor-alpha. J Biol Chem. 1994; 269:25057–61.
PMID:7929192

Supplementary Figures
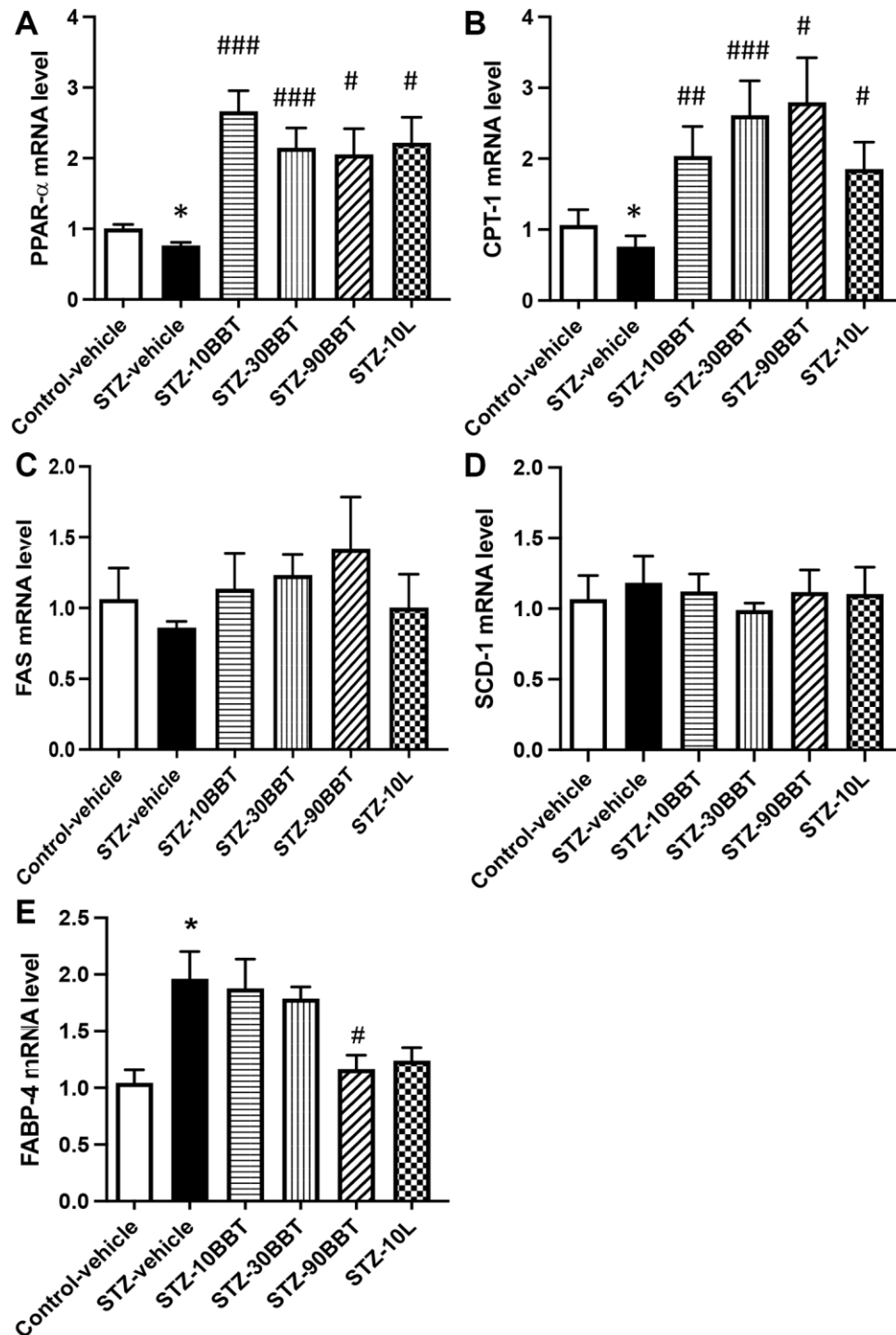
Supplementary Figure 1. BBT-877 reduces fat accumulation in the liver in STZ-induced diabetic mice. After treatment with BBT-877 for 8 weeks, mice were sacrificed, and their livers were collected. RNA was extracted and subjected to qRT-PCR for analyzing (**A**) PPAR-α, (**B**) CPT-1, (**C**) FAS, (**D**) SCD-1, and (**E**) FABP-4 expression levels. Abbreviations: STZ: streptozotocin; qRT-PCR: quantitative reverse transcriptase-polymerase chain reaction. STZ-10BBT contains 10 mg/kg of BBT-877; STZ-30BBT contains 30 mg/kg of BBT-877; STZ-90BBT contains 90 mg/kg of BBT-877; and STZ-10L contains 10 mg/kg of losartan. $^{*}p < 0.05$, control-vehicle vs. STZ-vehicle, $^{\#}p < 0.05$, STZ-vehicle vs. STZ-10, 30, 90BBT or STZ-10L, $n = 8$–10.
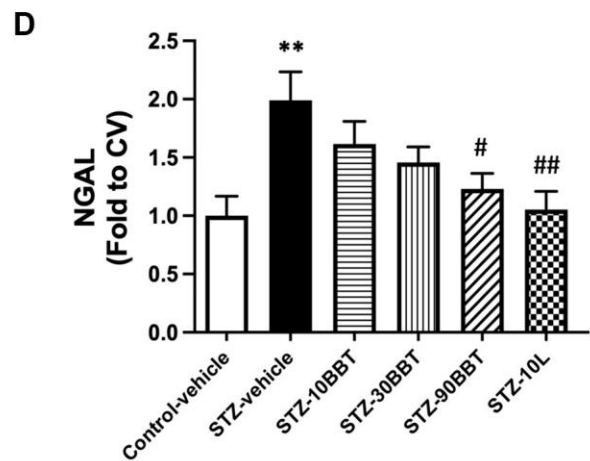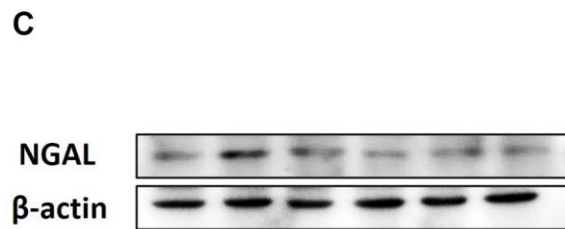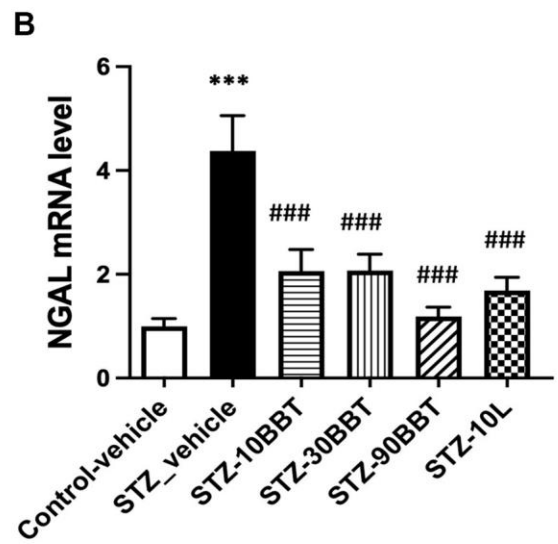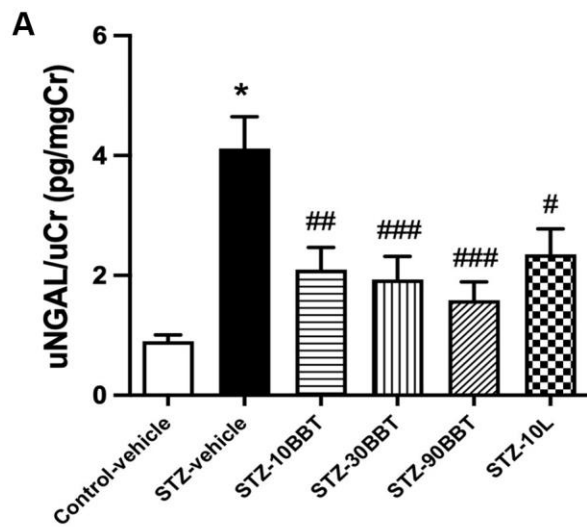
Supplementary Figure 2. BBT-877 reduces glomerular injury in the kidneys of STZ-induced diabetic mice. After treatment with BBT-877 for 8 weeks, urinary neutrophil gelatinase-associated lipocalin (NGAL) were measured. (**A**) Urinary NGAL level; (**B**) NGAL mRNA in kidney tissue; (**C**) Representative image; (**D**) Urinary NGAL protein level in kidney tissue. Abbreviation: STZ: streptozotocin. STZ-10BBT stands for BBT-877 10 mg/kg; STZ-30BBT stands for BBT-877 30 mg/kg; STZ-90BBT stands for BBT-877 90 mg/kg; and STZ-10L stands for losartan 10 mg/kg. *$p < 0.05$, control-vehicle vs. STZ-vehicle, #$p < 0.05$, STZ-vehicle vs. STZ-10, 30, 90BBT or STZ-10L, n = 8–10.